Bulletin of the Mineral Research and Exploration

http://bulletin.mta.gov.tr

# Rare Earth Element Potentials of Red-Colored Eocene Kazmaca and Late Eocene–Early Miocene İncik and Bayındır Formations (*Kırıkkale, Türkiye*)

Berna YAVUZ PEHLİVANLI[*a] and Menevşe ALTAN[b]

[a]*Yozgat Bozok University, Faculty of Engineering and Architecture, Department of Geological Engineering, Yozgat, Türkiye*
[b]*Graduate Student, Institute of Graduate Education, Yozgat Bozok University, Yozgat, Türkiye*

*Research Article*

Keywords:
Rare Earth Elements (REEs), Fourmarierite, Red Sedimentary Rocks, Kazmaca Formation, İncik Formation, Bayındır Formation.

**ABSTRACT**

Thered-colored sedimentary rocks of the Kazmaca, İncik, and Bayındır formations, particularly the red mudstones, exhibit noteworthy enrichment in Rare Earth Elements (REEs) and uranium. These fine-grained units were deposited in low-energy lacustrine to shallow-marine environments, where redox-sensitive geochemical processes played a central role in elemental mobilization and accumulation. Mineralogical and geochemical analyses, including XRD, XRF, and ICP-MS, identified the uranium-bearing mineral Fourmarierite, confirming the presence of uranium mineralization. This finding is supported by elevated Cu/Al ratios, increased Fe concentrations, and trace-element distributions indicative of a redox-controlled diagenetic environment. The high Fe concentrations and Cu/Al ratiosact as geochemical proxies for REE-hosting phases. The depositional setting, characterized by low dissolved oxygen levels, likely reflects a warm and humid paleoclimate that enhanced chemical weathering and facilitated the mobilization and subsequent precipitation of uranium and REEs. Notably, dark-colored mudstone interbeds within the sandstone sequences exhibit localized uranium accumulation, which may represent precursor zones for secondary REE mineralization. These findings underscore the importance of redox conditions and climatic factors in controlling REE and uranium enrichment in red bed sequences. The presence of Fourmarierite, in conjunction with distinctive geochemical signatures, suggests a significant potential for REE exploration in these formations.

*Received Date: 15.05.2025*
*Accepted Date: 27.10.2025*

## 1. Introduction

Rare Earth Elements (REEs) are essential components in modern high-technology applications, playing a critical role in sectors such as electronics, energy, defense, communication, and renewable energy (Chakhmouradianand Wall, 2012). Despite their relative abundance in the Earth's crust, economically viable REE concentrations are limited, with the majority of global production being derived from China, particularly from ion-adsorption deposits (IADs) (Sanematsu et al., 2013; Zeng et al., 2019; Zhu et al., 2022). These deposits are formed through intense chemical weathering of granitic and alkaline rocks in tropical to subtropical climates, where REEs become weakly adsorbed onto the surfaces of clay minerals (Yang et al., 1981; Bao and Zhao, 2008). Due to their amenability to low-cost leaching and minimal environmental disruption, IAD deposits are regarded as

Citation Info: Pehlivanlı, B. Y. and Altan, M. 2025. Rare Earth Element Potentials of Red-Colored Eocene Kazmaca and Late Eocene–Early Miocene İncik and Bayındır Formations (Kırıkkale, Türkiye). Bulletin of the Mineral Research and Exploration 178, 130-148. https://doi.org/10.19111/bulletinofmre.1811818

**Corresponding author: Berna YAVUZ, berna.yavuz@yobu.edu.tr*

both economically and ecologically favorable (Wang et al., 2018). In addition, they are often enriched in heavy REEs (HREEs) such as Dy, Tb, and Yb, which are critical for advanced technologies. However, the geochemical behavior of REEs in these systems is not yet fully understood, particularly with regard to their ion-exchangeable forms in weathering profiles, which may vary considerably from their total concentrations (Ding, 2012; Wang et al., 2018).

Beyond these classical settings, it has been suggested that red-bed sedimentary-type environments associated with uranium and copper sulfide deposits may also host REE enrichment (Lottermoser, 1990; Dill, 2010). In such environments, the reduction of sulfate to hydrogen sulfide ($H_2S$) by organic matter promotes the precipitation of copper sulfides, an important geochemical process linked to trace-metal concentration (Frondel, 1958; Jahn et al., 1981; Yavuz Pehlivanlı, 2019; 2022). Although red-bed systems are typically oxidizing and poor in organic matter and sulfide species, minor enrichments of elements such as Cu, U, V, Mo, and REEs may stil occur through mechanisms such as fluid migration, adsorption on to Fe-oxides, or secondary diagenetic processes (Möller, 1989; Dill, 2010). These environments therefore represent a less-explored, but potentially significant REE resource.

In this context, secondary uranium minerals, particularly Fourmarierite, have garnered attention due to their possible role in REE fractionation. Fourmarierite is a secondary uranium mineral formed through the alteration of uraninite ($UO_2$) under surface- or near-surface oxidative conditions (Frondel, 1958; Finch and Murakami, 1999). Its presence indicates that primary uranium enrichment has occurred in the region and that subsequent oxidative processes have modified the mineralization. The transformation of uraninite into Fourmarierite requires the mobilization of uranium as uranyl ions ($UO_2^{2+}$), followed by reprecipitation under favorable pH and redox conditions (Langmuir, 1978; Wronkiewicz and Buck, 1996). As a result, Fourmarierite often forms in environments affected by groundwater movement and may serve as a surface indicator of subsurface uranium enrichment (Dahlkamp, 1993; Cuney and Kyser, 2009).

Recent studies suggest that secondary uranium minerals such as Fourmarierite and Becquerelite can exhibit distinct REE fractionation patterns during the alteration of uraninite, highlighting their role as potential REE traps (Larson et al., 2017; Xiong and Wang, 2018). For example, oxidizing conditions have been shown to promote the enrichment of light REEs (LREEs) in secondary uranium-oxide-hydrates. Under reducing to weakly oxidizing conditions, interactions between fluids and uraninite can further mobilize and selectively precipitate REEs alongside U(VI) phases. Thus, the formation of Fourmarierite may reflect not only uranium remobilization but also localized REE enrichment, which has important implications for both uranium exploration and the identification of critical metal resources.

Therefore, this study investigates the geochemical potential of both ion-adsorption-type and red-bed-type formations, with a focus on the distribution, behavior, and fractionation of heavy rare earth elements (HREEs), especially in association with secondary uranium minerals such as Fourmarierite.

## 2. General Geology and Stratigraphy

The basement of the study area is composed of ophiolitic mélange, which is intruded by the Paleocene-aged Sulakyurt granite. The Sulakyurt granite consists of tonalite and gabbro-diorite, with mafic microgranular enclaves observed within the tonalite. This granite is unconformably overlain by the younger İncik and Kızılırmak formations. The youngest units in the region are Quaternary alluvial deposits.

The İncik Formation, dated to the Late Eocene–Early Miocene, comprises various lithologies such as reddish-brown conglomerate, marl, carbonate, gypsum, and sandstone. It was deposited in a continental and partially marine environment and is characterized by its rich plant fossil content and the presence of evaporite minerals.

Overlying this unit with angular unconformity is the Kızılırmak Formation, which is Late Miocene in age. Within this formation, contemporaneous Faraşlı volcanics are interbedded, consisting mainly of basaltic compositions.

The Bayındır Formation, formed during the Late Oligocene–Early Miocene interval, is characterized by evaporitic features and carbonate-rich deposits such as gypsum, dolomite, limestone, and marl. The sedimentary structures with volcanic input and the presence of extensive evaporite layers indicate deposition under arid to semi-arid climatic conditions.

The Kazmaca Formation is Eocene in age and developed within a fault-controlled asymmetric graben basin. It consists of sedimentary rocks such as mudstone, claystone, nummulitic limestone, and carbonaceous shale. Within this formation, coal, laterite, and rare-element accumulations are found. The formation was influenced by fluvial, lacustrine, and marine depositional environments (Figures 1–3).

## 3. Materials and Methods

In this study, a total of 45 samples were collected from red-colored rocks (generally silty sandstone and mudstone) belonging to various geological units around Kırıkkale, and 30 of these samples were selected for laboratory analyses (Table 1; Figures 4–5).

To determine the mineralogical and chemical compositions of the samples, X-Ray Diffraction (XRD), X-Ray Fluorescence Spectrometry (XRF), and Inductively Coupled Plasma Mass Spectrometry (ICP-MS) methods were employed. All analyses were conducted at the BİLTEM laboratories of Yozgat Bozok University.

Prior to laboratory processing, the samples were dried at 110°C for 24 hours, then broken into smaller pieces using a hammer and a jaw crusher. The crushed samples were subsequently ground in a disc mill and sieved to a grain size of 63 microns to prepare them for analysis.

XRD analyses were conducted on 20 powdered samples to determine mineral types. The samples were placed into the sample holders, and the resulting data were evaluated using the Rietveld refinement method with the HighScore Plus software.

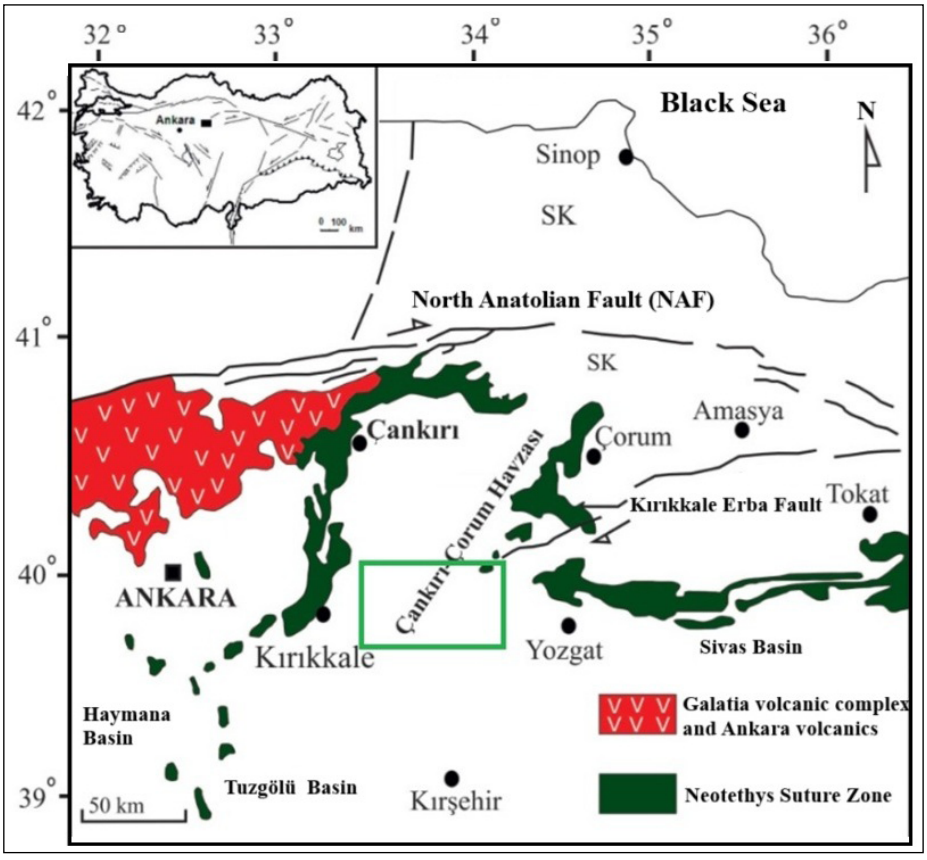


Figure 1- Location map of the study area (Karadenizli, 1999; Karadenizli et al., 2004).

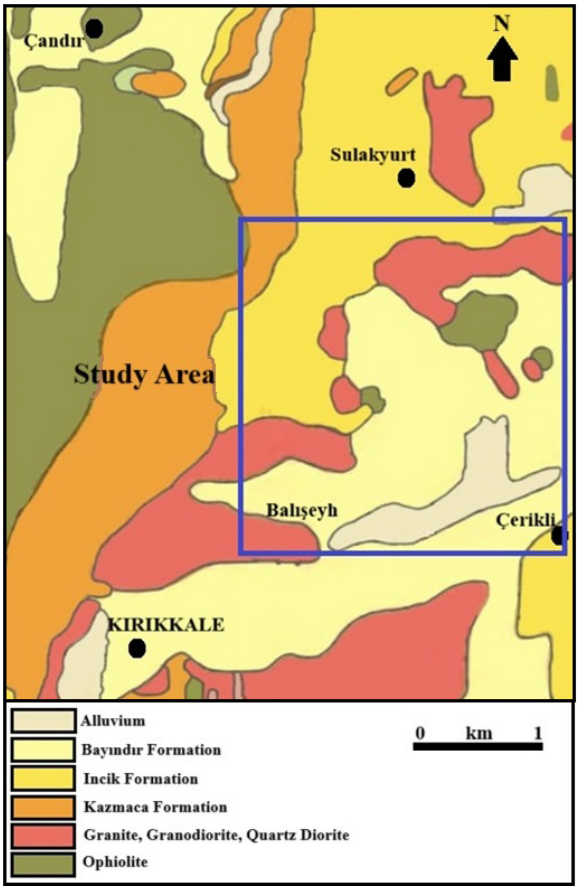


Figure 2- Geological setting of the Kırıkkale region (Yoldaş, 1982; Hakyemez et al., 1986; MTA, 2002).

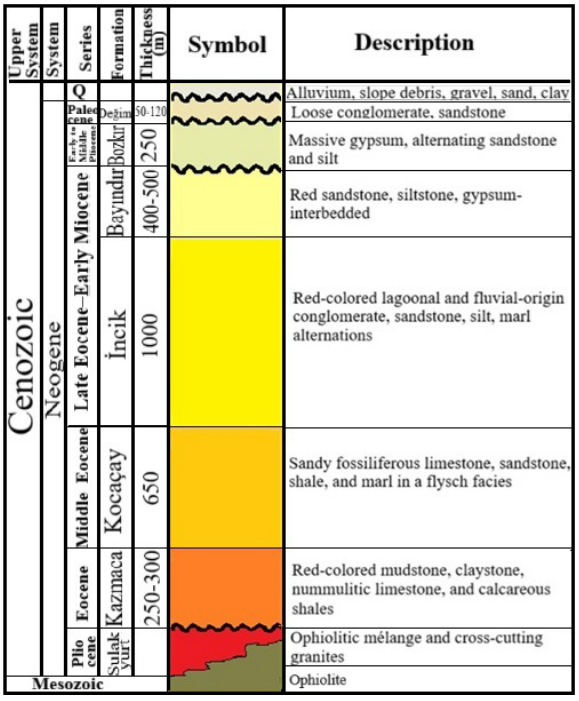


Figure 3- Generalized stratigraphic column of the rock units in the study area (adapted and revised from Birgili et al., 1975; Yoldaş, 1982; Hakyemez et al., 1986).

Table 1-Sampling locations of red-colored outcropping rocks in the Kırıkkale region.

| Formation Name | Formation Age | SampleCodes |
|---|---|---|
| Bayındır Formation | Late Eocene–Early Miocene | BAY (1-6)<br>ÇER (1-6)<br>AKC (1-7) |
| İncik Formation | Late Eocene–Early Miocene | INC (1-5)<br>FAR (1-5) |
| Kazmaca Formation | Eocene | KAZ (1-15) |

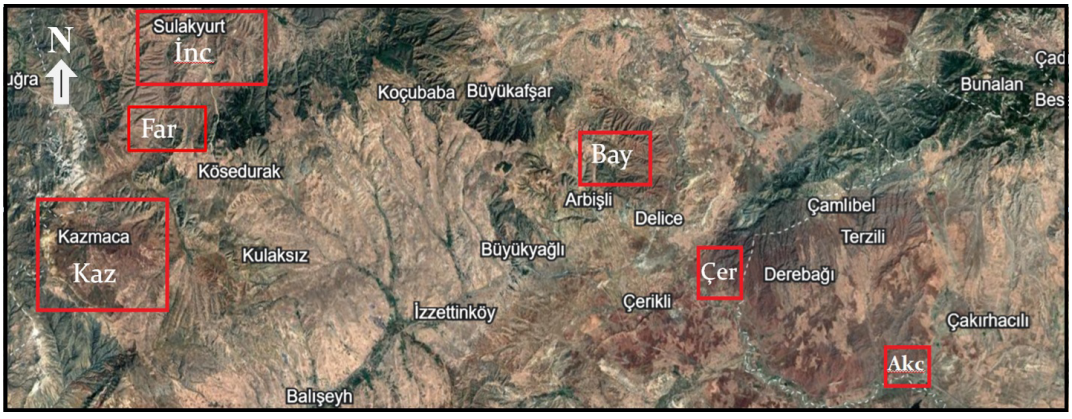


Figure 4- Location of the sampled section on the satellite image.

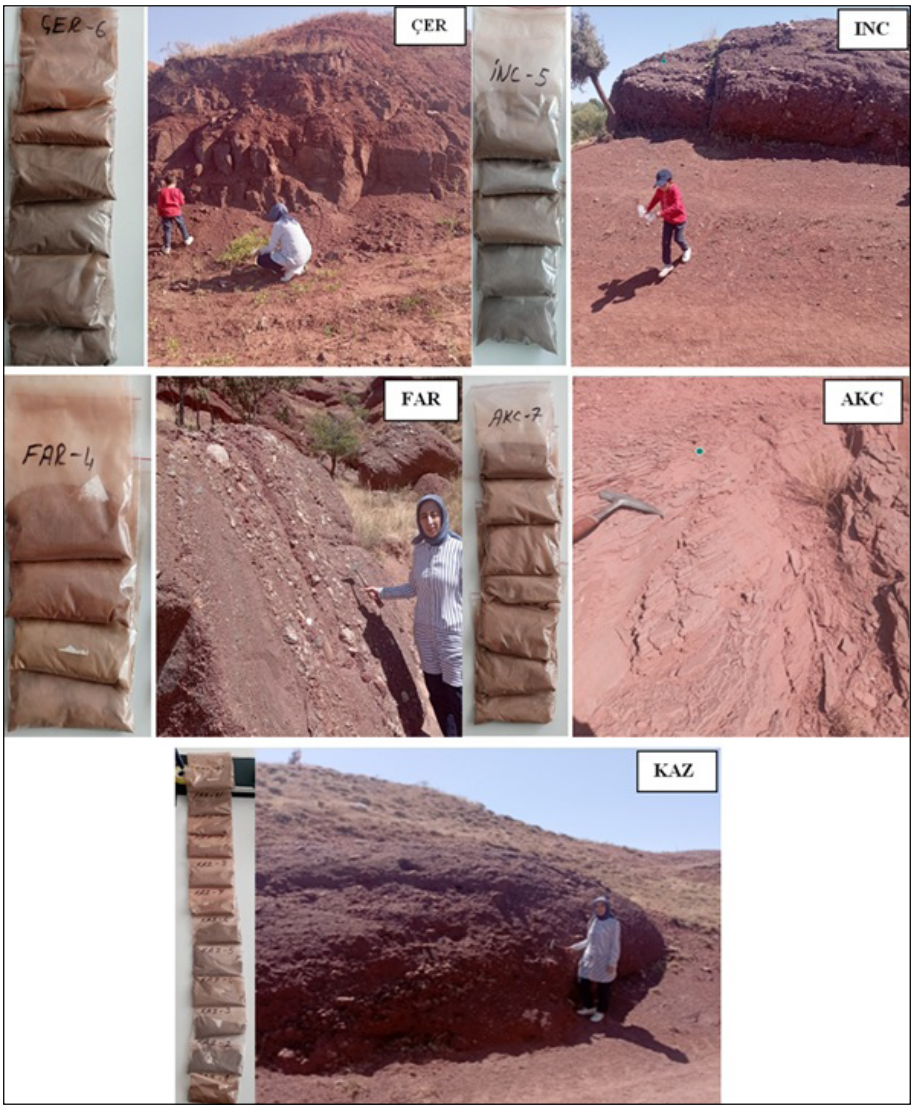


Figure 5-Samples collected from the Bayındır, İncik, and Kazmaca formations.

XRF analyses were used to determine the major and trace element contents of the rocks. A total of 30 samples were mixed with a binding agent, pressed into pellets, and analyzed using a PANalytical Axios MAX instrument. The data were processed using SuperQ software, and the analyses were calibrated against international reference standards.

ICP-MS analyses were performed to investigate rare earth elements (REEs) and trace elements. Thirty powdered samples were dissolved in a 1%$HNO_3$ solution and heated, followed by filtration and analysis using an Agilent 7500a ICP-MS instrument. The measurement results were evaluated using the MassHunter software.

As a result of these analytical procedures, the mineral and elemental compositions of red-colored rocks around Kırıkkale were comprehensively identified.

## 4. Discussion

### 4.1. General Evaluation of Mineral Contents

The mineralogical compositions of the rock samples collected from the study area were determined through XRD analyses (Table 2). The results reveal that the majority of the samples are composed of quartz, carbonate minerals (particularly dolomite), feldspar, and clay minerals, which are typical components of sedimentary rocks. In addition to these

Table 2- Common XRD data for all samples from the study area.

| Mineral | Chemical Formula |
|---|---|
| Albite | $NaAlSi_3O_8$ |
| Amesite | $(Mg_2Al)(SiAlO_5)(OH)_4$ |
| Amphibole | $(Mg_2Al)(SiAlO_5)(OH)_4$ |
| Analcime | $NaAlSi_2O_6.H_2O$ |
| Andesine | $(Na, Ca)(Al, Si)_4O_8$ |
| Calcite | $CaCO_3$ |
| Chlorite | $(Mg, Fe)_3(Si, Al)_4O_{10}(OH)_2.(Mg, Fe)_3(OH)_6$ |
| Clinochlore | $(Mg, Fe)_5Al(Si_3Al)O_{10}(OH)_8$ |
| Clinopyroxene (Ca, Zn) | $Ca(Mg, Fe, Al)(Si, Al)_2O_6$ or, ifreplacedbyZn, $Ca(Zn, Fe)(Si, Al)_2O_6$ |
| Dolomite | $CaMg(CO_3)_2$ |
| Enstatite | $Mg_2Si_2O_6$ |
| Fourmarierite | $PbU_4O_6(OH)_4.5H_2O$ |
| Gypsum | $CaSO_4.2H_2O$ |
| Illite | $K_{0\cdot65}Al_2Al_{0\cdot65}Si_{3\cdot35}O_{102}$ |
| Kaolinite | $Al_2Si_2O_5(OH)_4$ |
| Lizardite | $Mg_3Si_2O_5(OH)_4$ |
| Mica, containinglithium | $KAl_2(AlSi_3O_{10})(OH)_2$ |
| Montmorillonite | $(Na, Ca)_{0\cdot3}(Al, Mg)_2Si_4O_{10}(OH)_2.nH_2O$ |
| Muscovite | $KAl_2(Si_3Al)O_{10}(OH)_2$ |
| Palygorskite | $(Mg, Al)_2Si_4O_{10}(OH).4(H_2O)$ |
| Quartz | $SiO_2$ |
| Na-Anorthite | $(Na, Ca)AlSi_3O_8$ |
| Vermiculite | $(Mg, Fe^{2+}, Fe^{3+})_3(Si, Al)_4O_{10}(OH)_2.4H_2O$ |
| Zeolite X, Pb-changeable | $Na_{86}Al_{86}Si_{106}O_{384}.264H_2O$ |

common phases, the rare secondary uranyl mineral Fourmarierite was detected in some samples.

Fourmarierite, a hydrated lead-uranate compound, typically forms under oxidizing conditions in uranium-enriched environments and is indicative of oxidation zones. Its occurrence is often associated with weakly acidic and oxidizing conditions within carbonate-rich settings.

Interestingly, although the general geochemical setting reflects oxidizing conditions conducive to uranyl mineral formation, evidence such as minor occurrences of hydrogen sulfide ($H_2S$) and a relative depletion of organic matter point to localized reducing microenvironments. This suggests a complex redox regime possibly related to diagenetic fluid migration and fluctuating redox boundaries.

Beyond these classical settings, it has been suggested that red-bed-type sedimentary environments, often associated with uranium and copper sulfide deposits, may also exhibit rare earth element (REE) enrichment (Lottermoser, 1990; Dill, 2010). In such systems, the microbial reduction of sulfate to hydrogen sulfide ($H_2S$) by residual organic matter can lead to the precipitation of copper sulfides, an important geochemical process for concentrating trace metals such as Cu, U, V, Mo, and REEs (Frondel, 1958; Jahn et al., 1981; Yavuz Pehlivanlı, 2019; 2022). Although these environments are generally oxidizing and low in organic carbon and sulfide species, minor enrichments may still occur

via mechanisms such as fluid migration, adsorption onto Fe-oxides, or secondary diagenetic processes (Möller, 1989; Dill, 2010). Thus, these systems may represent an underexplored but potentially significant metallogenic and REE-bearing environment.

4.2. Elemental Contents

Based on the elemental analyses conducted on the rock samples collected from the field, the variations in elemental concentrations with depth were evaluated for each sampling point, and elements exhibiting similar trends were grouped accordingly (Figures 6-14).

Group 1 (High Mobility/Evaporitic): Pd, Na, and B show similar distribution patterns, likely influenced by surface-related mobilization processes or evaporitic conditions due to their relatively high mobility in surface and near-surface environments (Wedepohl, 1995, Figure 6).

Group 2 (Low Mobility/Resistant Minerals): Zr, Bi, Tl, and Sn, typically low-mobility elements associated with heavy metal-bearing accessory minerals, likely reflect common sources related to mineral weathering and resistance to chemical alteration (Alloway, 2013, Figure 7).

Group 3 (Aluminosilicate Control): The grouping of Th, Al, Ga, K, Cs, and Rb suggests a strong association with clay minerals and feldspars, indicating resistance to chemical weathering and control by aluminosilicate phases (Rollinson, 1993; Kabata-Pendias and Pendias, 2011, Figure 8).

Group 4 (Biophilic/Phosphate): Cd, As, Zn, Ca, and P, known for their biophilic behavior, likely reflect interactions with organic matter and phosphate minerals, Figure 9a).

Group 5 (Redox-Influenced REEs): Mg, V, Eu, and Sm show behavior influenced by redox conditions and early diagenetic mobility typical of rare earth elements (Dill, 2010, Figure 9b).

Group 6 (Redox-Sensitive/Co-Migration): In, Fe, Mn, and Y are sensitive to redox changes and tend to co-migrate under oxidizing conditions (Figure 10a).

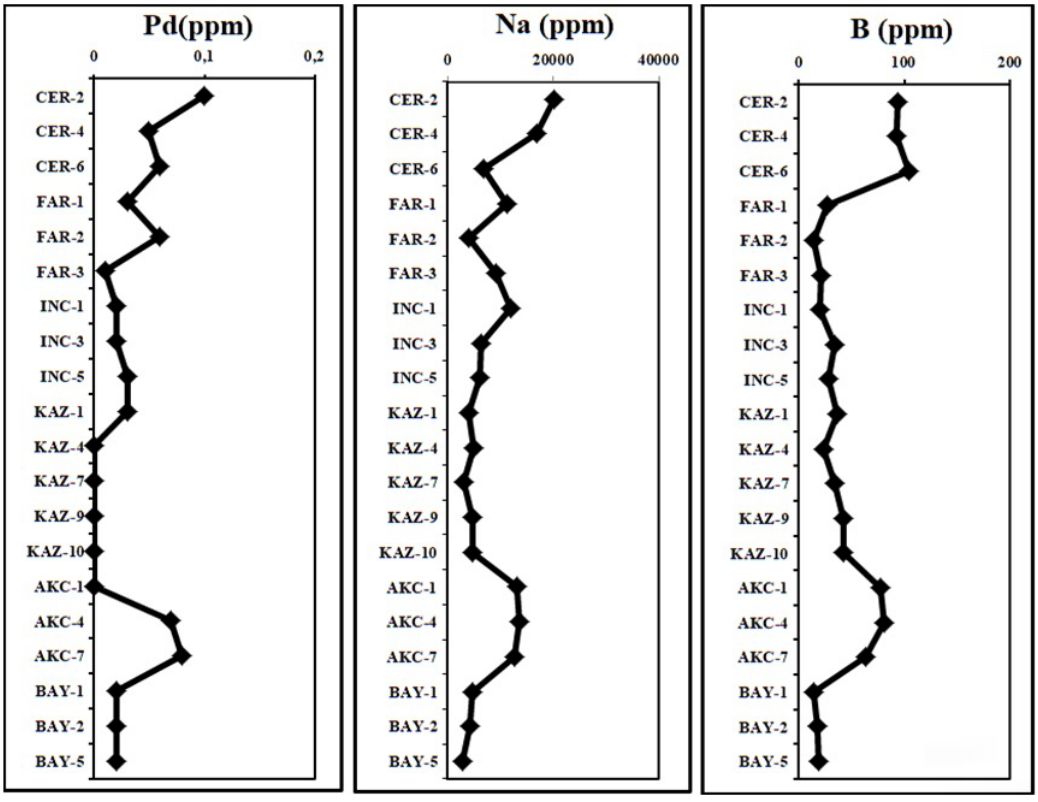


Figure 6- When examining the variations of elements with depth, elements displaying similar trends were grouped together. Pd, Na, and B exhibit similar patterns (Group 1).

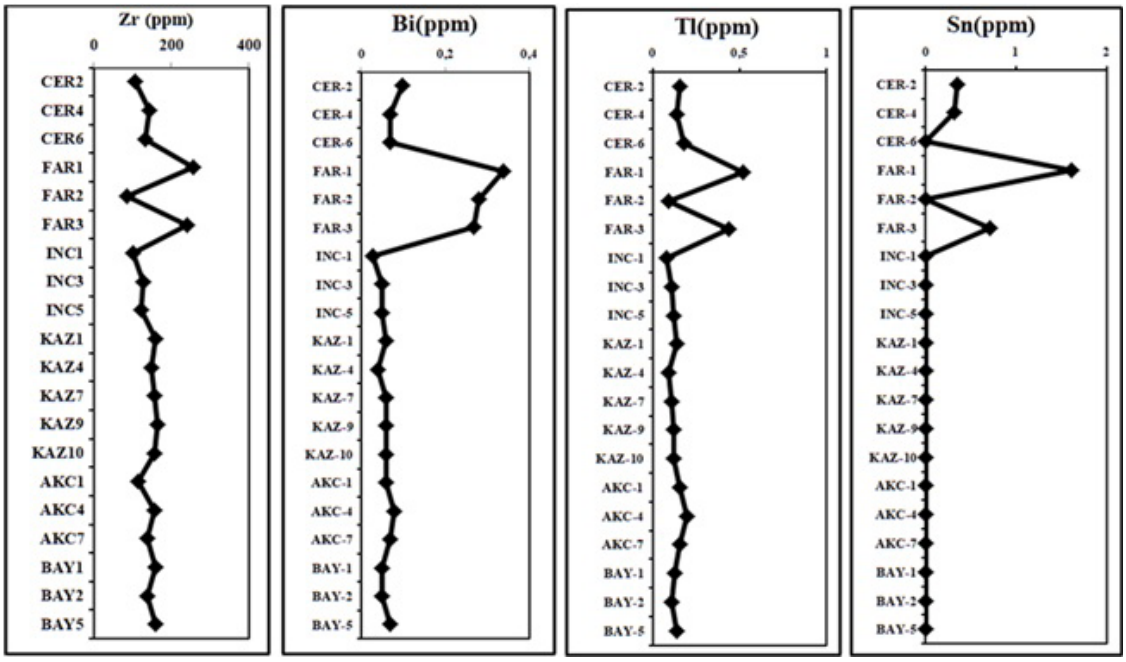


Figure 7- When examining the variations of elements with depth, elements displaying similar trends were grouped together. Zr, Bi, Tl, and Sn exhibit similar patterns (Group 2).

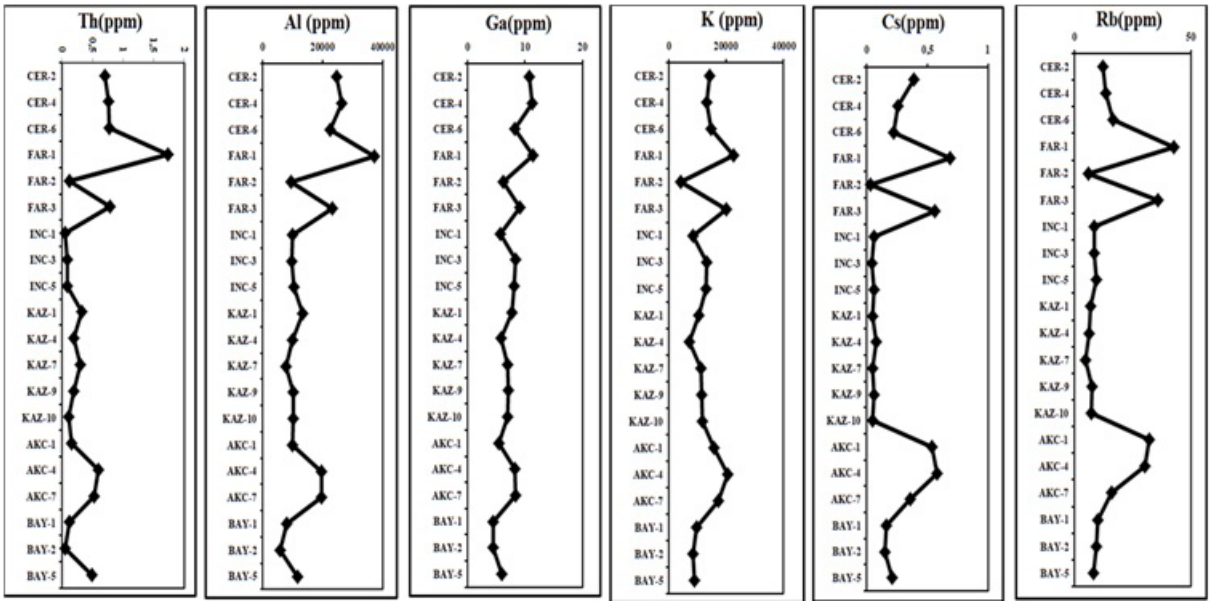


Figure 8- The grouping of elements showing similar variation trends with depth was carried out. Th, Al, Ga, K, Cs, and Rb exhibit similar patterns (Group 3).

Group 7 (Immobile/Fixed Phases): Ge, Pb, Sc, and Sb are relatively immobile and tend to remain fixed in stable mineral phases (Brookins, 1988; Lottermoser, 2010, Figure 10b)

Group 8 (Light REEs): The group consisting of La, Nd, Pr, and Ce represents light rare earth elements (LREEs), which often adsorb onto Fe-oxides or incorporate into carbonate phases, resulting in similar geochemical behavior (Henderson, 1984; Möller, 1989, Figure 11).

Group 9 (Redox Mobile/Diagenetic Fluids): Mo, U, Ta, Li, and Ti are redox-sensitive elements that tend

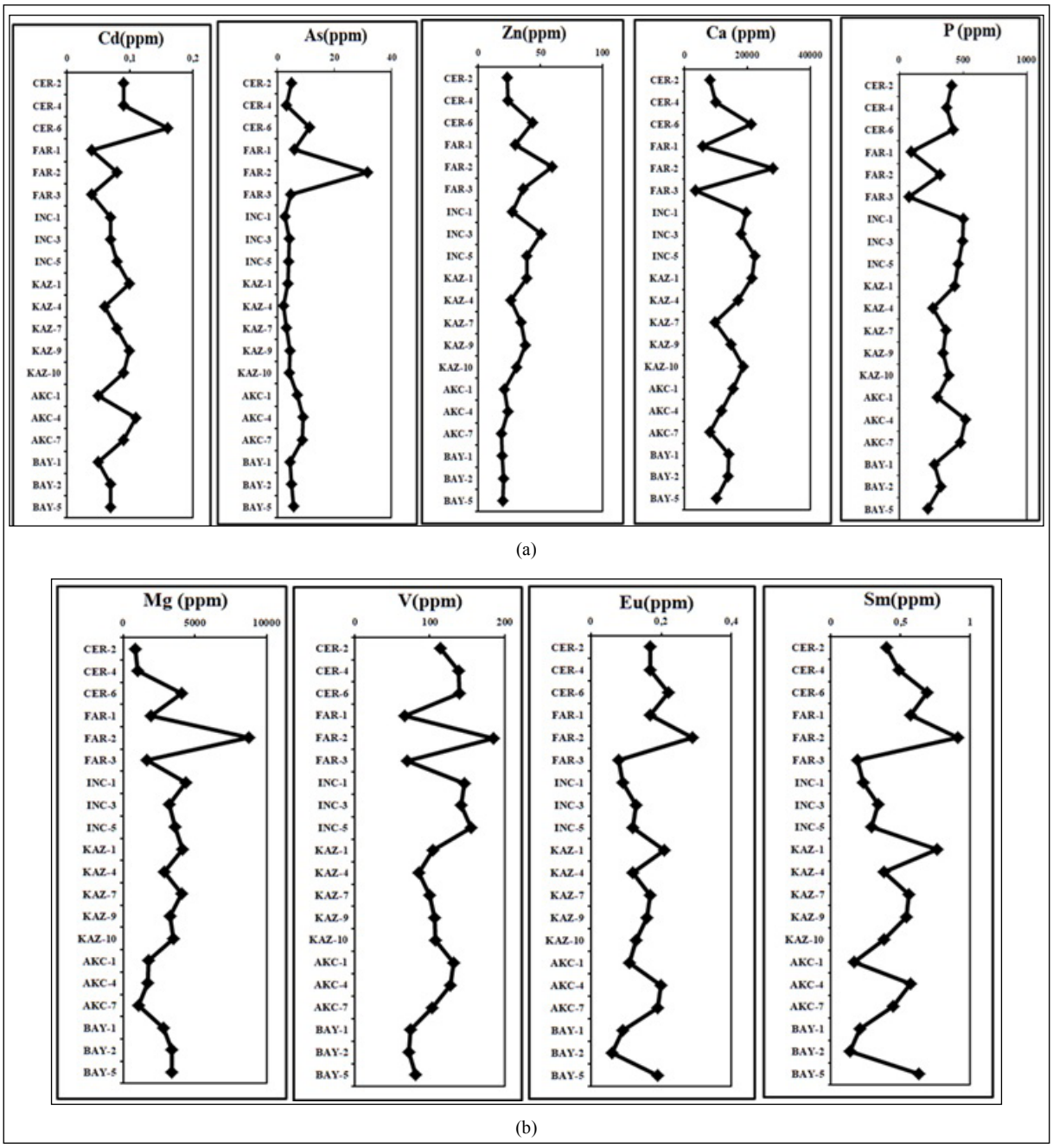


Figure 9- The grouping of elements showing similar variation trends with depth was carried out. a) Group 4 (Cd, As, Zn, Ca, and P) and b) Group 5 (Mg, V, Eu, and Sm) exhibit similar patterns.

to become mobile under oxidizing conditions and may be redistributed through diagenetic fluids (Brookins, 1988; Cuney and Kyser, 2009, Figure 12).

Group 10 (Carbonate Affinity): Ba and Sr, which show strong affinity for carbonate phases, exhibit parallel patterns likely related to primary or secondary precipitation processes (Wedepohl, 1995, Figure 13).

Group 11 (Mafic/Ultramafic Weathering): Lastly, Ni and Cr display similar trends, often associated with the weathering of ultramafic or mafic lithologies (Rollinson, 1993, Figure 14).

These elemental groupings provide critical insights into the diversity of geochemical processes across the study area and the differential behavior of trace elements in relation to lithology, redox conditions, and

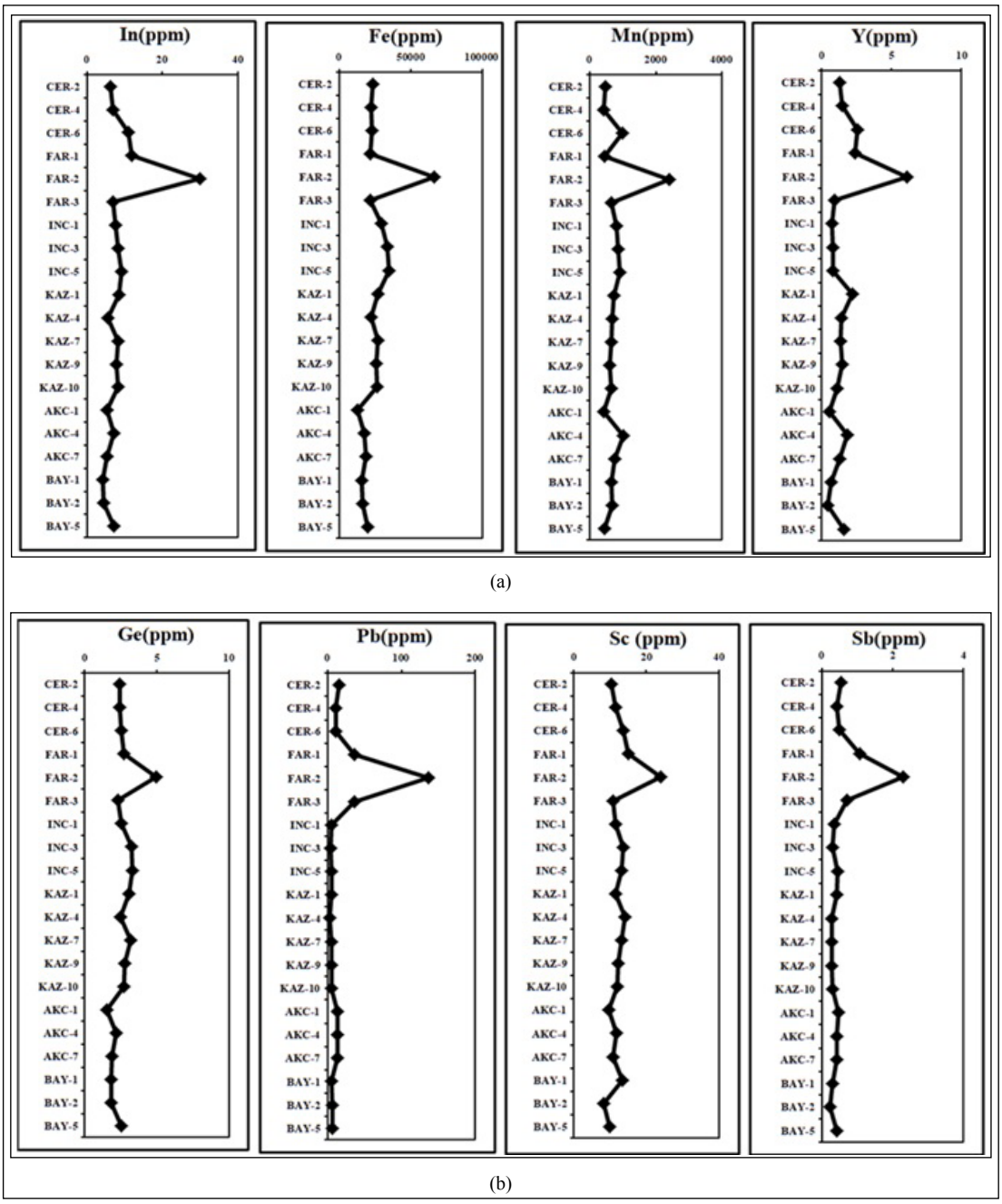


Figure 10- The grouping of elements showing similar variation trends with depth was carried out. a) Group 6 (In, Fe, Mn, and Y) and b) Group 7 (Ge, Pb, Sc, and Sb) exhibit similar patterns.

mineral associations (Price et al., 1991; Morteani and Preinfalk, 1996; Kynicky et al., 2012).

The abundance levels of elements from all sampling points assessed within the scope of the study were evaluated (Figures 15-20).

The abundance rankings of elements from different areas show significant variability among the sample points. For instance, in the Çerikli area, major elements such as Al, Fe, Na, K, and Ca display the highest abundances. Similarly, in the Faraşlı area, Fe, Al, K, Ca, and Na dominate. In samples from the İncik Formation, Fe, Ti, and Ca are the most abundant, while in the Kazmaca Formation, Fe, Ti, Ca, and K stand out. The Akçakent area is characterized by high levels of K, Fe, and Al, whereas in the Bayındır Formation,

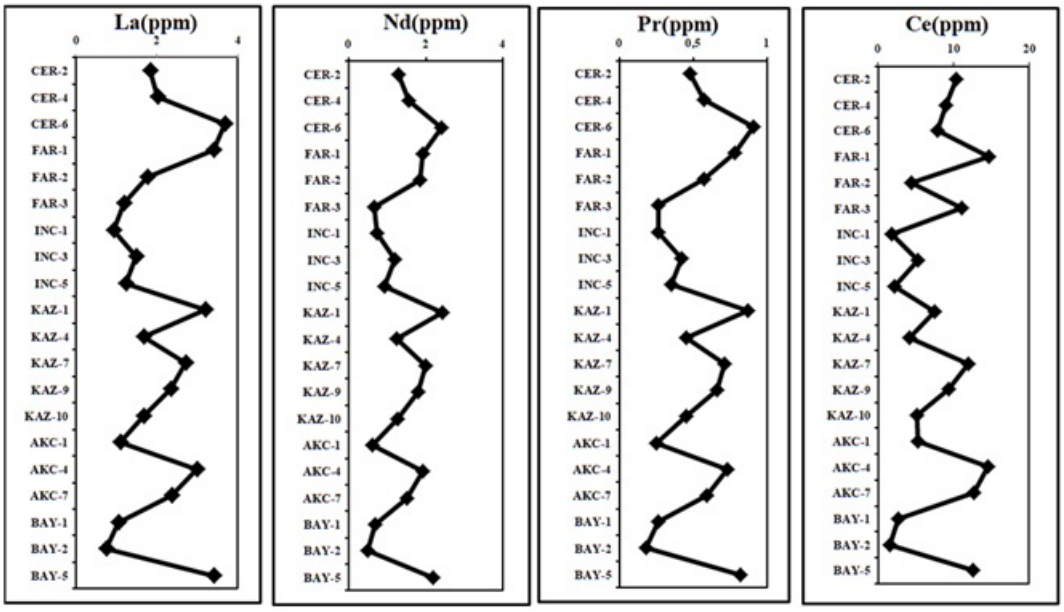


Figure 11- Thegrouping of elements show ing similar variation trends with depth was carried out. La, Nd, Pr, and Ce exhibit similar patterns (Group 8).

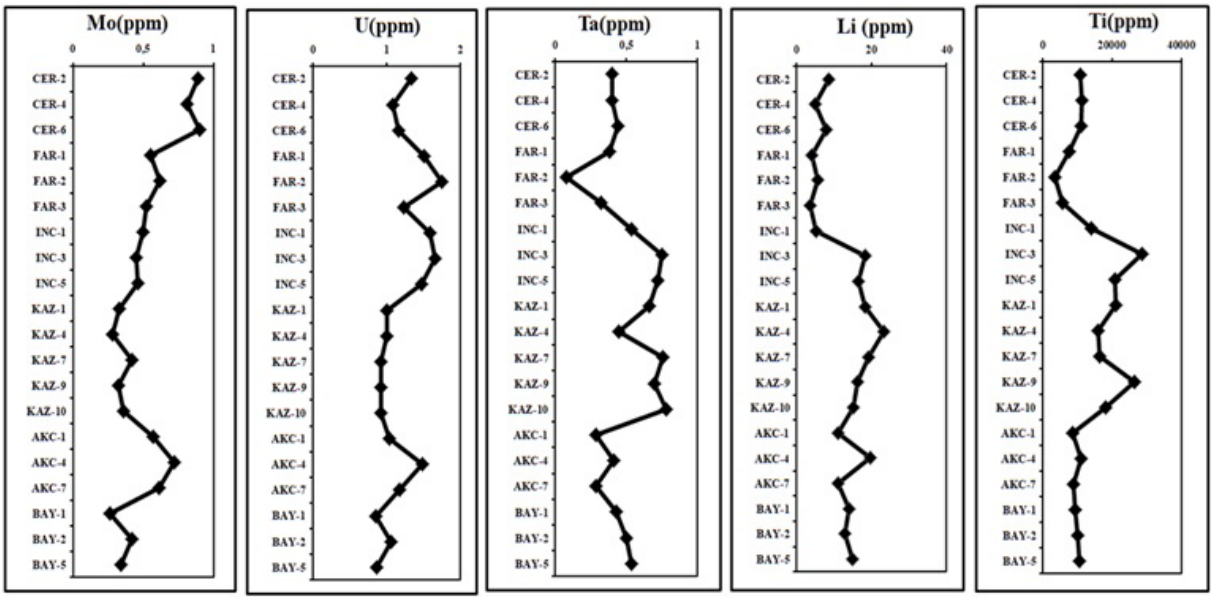


Figure 12- The grouping of elements showing similar variation trends with depth was carried out. Mo, U, Ta, Li, and Ti exhibit similar patterns (Group 9).

Fe, Ca, and Ti are the most dominant elements. The detailed abundance rankings of trace and rare earth elements (REEs) elements for each location are presented in Figure 15-20.

The analyses reveal notable variations in the abundance of rare earth elements (REEs) and uranium (U) across different sampling areas. In all regions, light rare earth elements (LREEs), such as Ce, La, and Nd, are found in high concentrations, while heavy rare earth elements (HREEs), including Lu, Tm, and Ho, typically appear in the lowest abundance ranks.

Particularly in the Çerikli, Faraşlı, İncik, and Bayındır formations, LREE enrichment is accompanied by a significant presence of uranium,

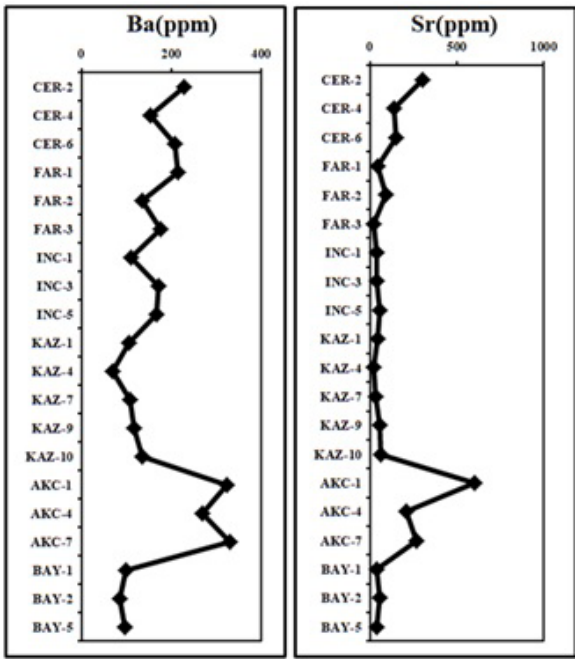


Figure 13- The grouping of elements showing similar variation trends with depth was carried out. Ba and Sr exhibit similar patterns (Group 10).

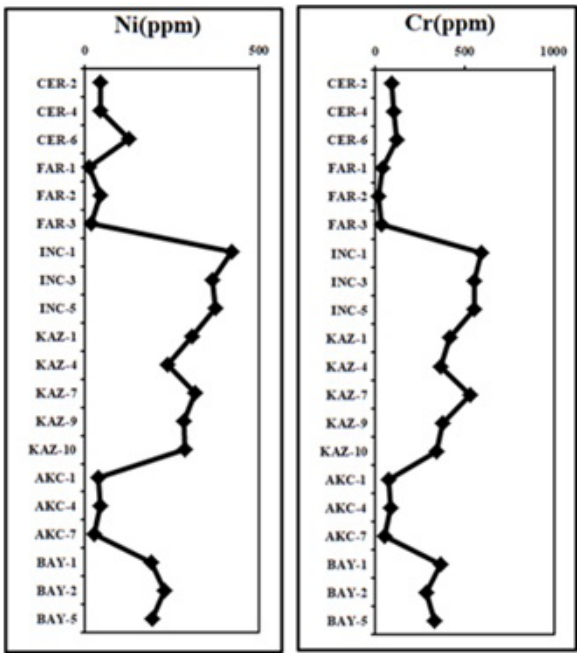


Figure 14- The grouping of elements showing similar variation trends with depth was carried out. Ni and Cr exhibit similar patterns (Group 11).

with U often ranked just after Ce and La. This indicates a strong potential for uranium accumulation in these formations. Similarly, in the Akçakent and Kazmaca areas, LREE dominance is observed alongside moderate to high uranium content. Overall, all studied formations display a clear LREE-enriched signature, and the co-enrichment of uranium further highlights their significance as promising targets for both REE and uranium exploration (Figure 15-20).

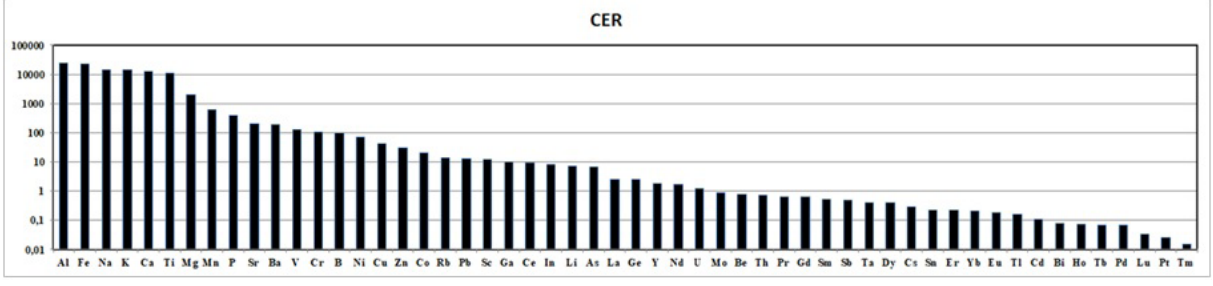


Figure 15-The element abundance ranking of the samples collected from the Çerikli area.

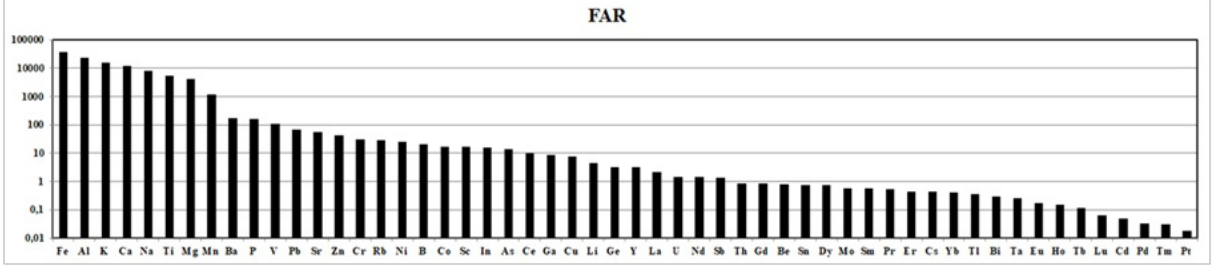


Figure 16-The element abundance ranking of the samples collected from the Faraşlı area.

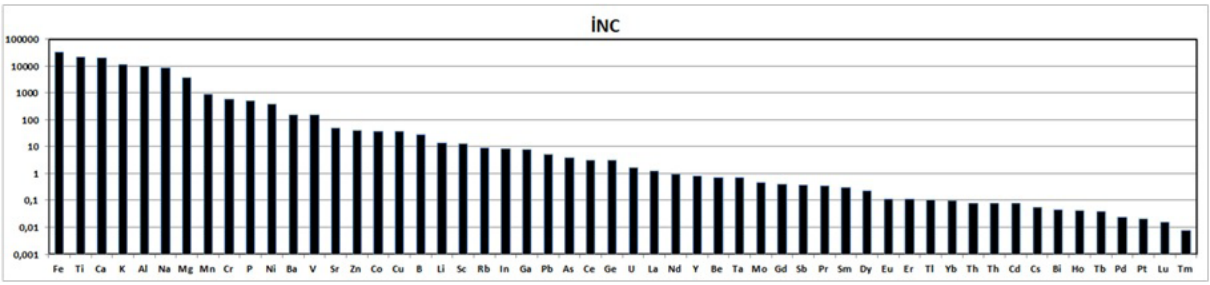


Figure 17-The element abundance ranking of the samples collected from the İncik area.

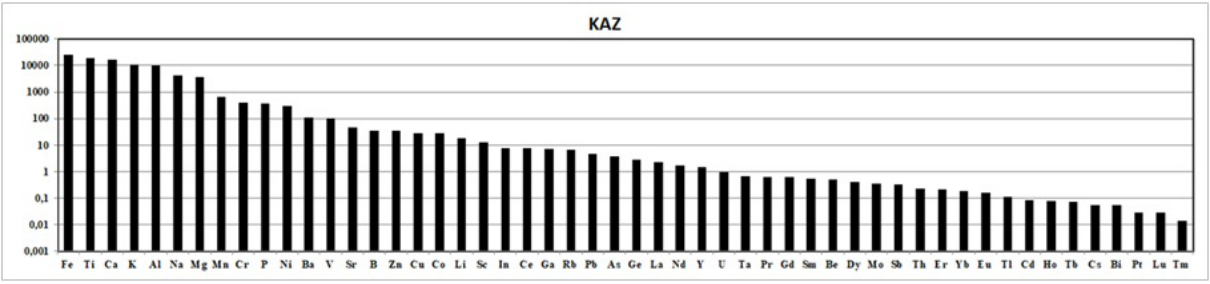


Figure 18-The element abundance ranking of the samples collected from the Kazmaca area.

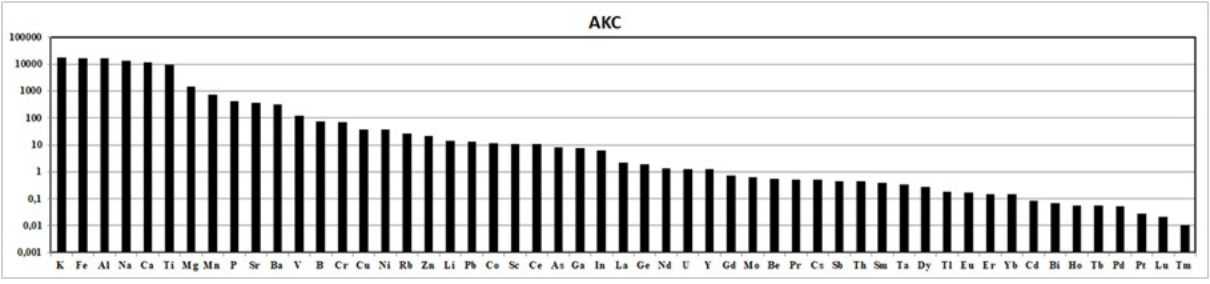


Figure 19- The element abundance ranking of the samples collected from the Akçakent area.

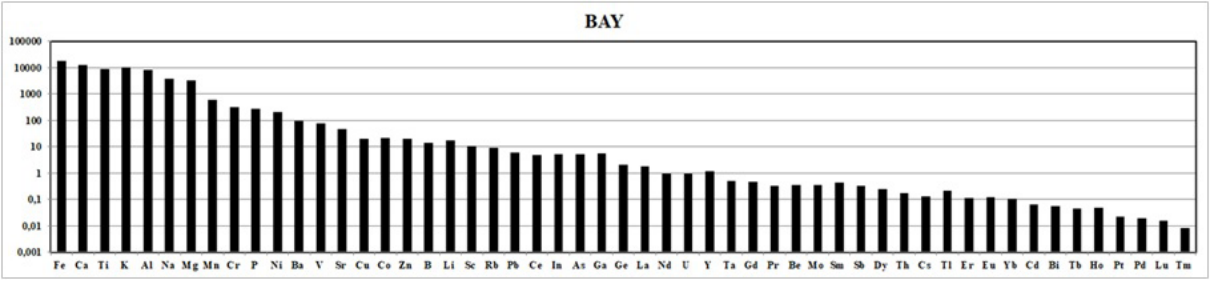


Figure 20- The element abundance ranking of the samples collected from the Bayındır area.

### 4.3. Rare Earth Elements

When the rare earth element (REE) contents are analyzed, a comparison among the Çerikli, Faraşlı, İncik, Kazmaca, Akçakent, and Bayındır units indicates that FAR−2 has the highest concentration in terms of total rare earth element (ΣREE) contents.

However, when the samples are evaluated group by group, it is observed that CER−6 in the Çerikli unit, FAR−2 in the Faraşlı unit, INC−3 in the İncik Formation, KAZ−1 in the Kazmaca Formation, AKC−4 in the Akçakent unit, and BAY−5 in the Bayındır Formation contain higher total rare earth element (ΣREE) concentrations.

Moreover, when examining the light rare earth elements (LREEs), a similar pattern emerges. Heavy rare earth elements (HREEs) also show similar characteristics to the medium rare earth elements (MREEs). For the MREEs, KAZ−7 displays higher concentrations, whereas for the HREEs, KAZ−7 again records the highest concentrations compared to others samples. In terms of total LREEs (ΣLREE), KAZ−1 exhibits the highest concentration (Figure 21-24; Table 3).

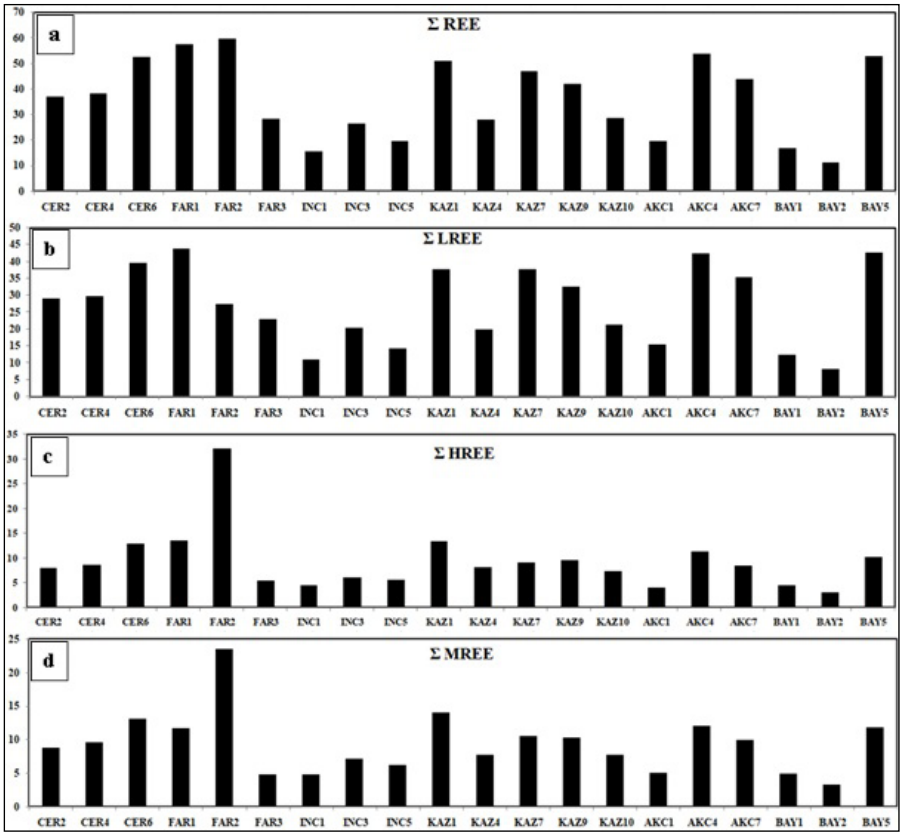


Figure 21- Comparison of, a) ΣREE, b) ΣLREE, c) ΣHREE, d) ΣMREE in all samples from the study area.

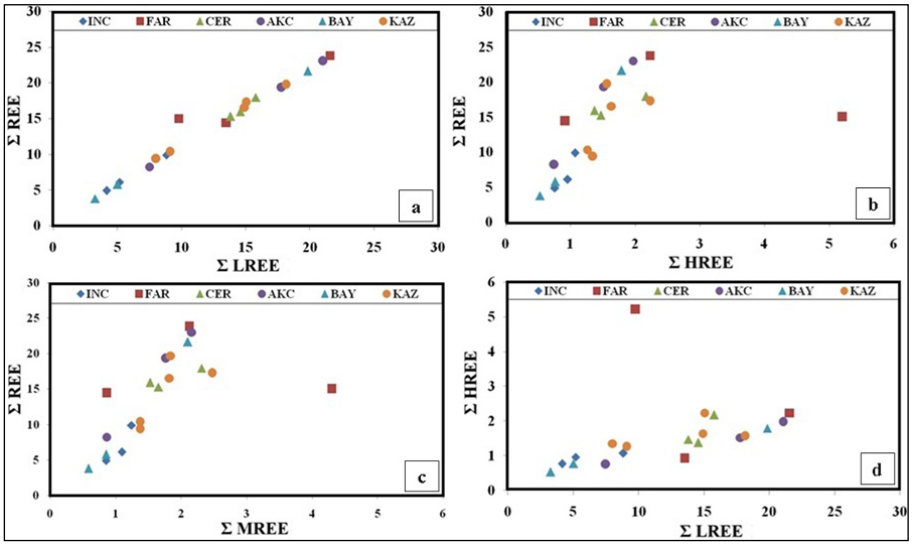


Figure 22- Comparison of a) ΣREE vs. ΣLREE (Light), b) ΣREE vs. ΣHREE (Heavy), c) ΣREE vs. ΣMREE (Medium), d) ΣHREE vs. ΣLREE.

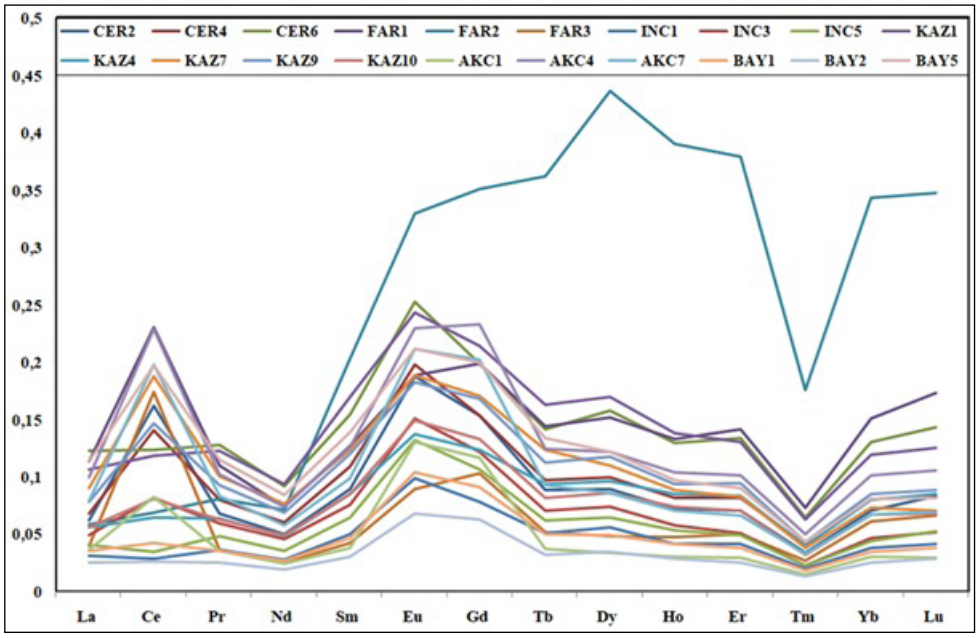


Figure 23- UCC-normalized REE patterns of all samples.

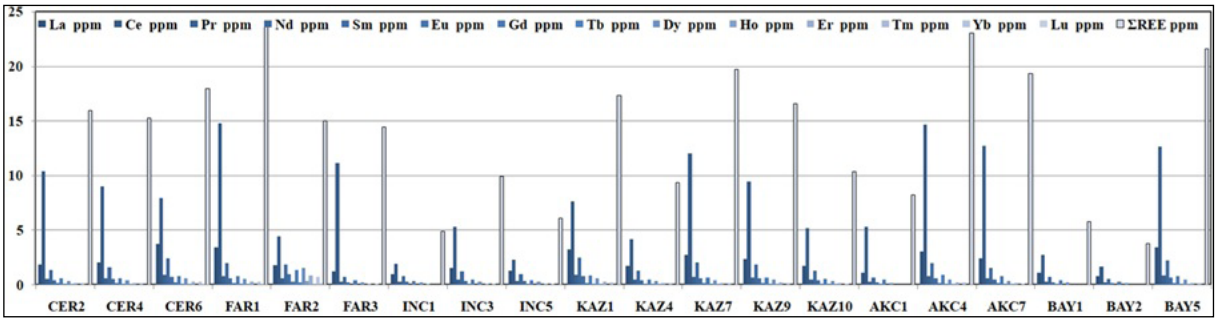


Figure 24- REE abundance comparison graph of samples from all sampling points.

Table 3-Average reference values for rare earth elements (REEs) (Boynton, 1984).

| REEs | PAAS (mean) | Average Shale | PAAS | Chondrite | Upper Crust | NASC |
|---|---|---|---|---|---|---|
| **La** | 44. 56 | 41 | 38. 2 | 0. 31 | 30 | 33. 04 |
| **Ce** | 88. 25 | 83 | 79. 6 | 0. 808 | 64 | 70. 5466 |
| **Pr** | 10. 15 | 10. 1 | 8. 83 | 0. 122 | 7. 1 | 8. 7 |
| **Nd** | 37. 32 | 38 | 33. 9 | 0. 6 | 26 | 31. 76 |
| **Sm** | 6. 884 | 7. 5 | 5. 55 | 0. 195 | 4. 5 | 5. 994 |
| **Eu** | 1. 215 | 1. 61 | 1. 08 | 0. 0735 | 0. 88 | 1. 3826 |
| **Tb** | 6. 884 | 6. 35 | 4. 66 | 0. 259 | 3. 8 | 5. 5025 |
| **Gd** | 0. 8914 | 1. 23 | 0. 774 | 0. 0474 | 0. 64 | 0. 94 |
| **Dy** | 5. 325 | 5. 5 | 4. 66 | 0. 322 | 3. 5 | 5. 54 |
| **Ho** | 1. 053 | 1. 34 | 0. 991 | 0. 0718 | 0. 8 | 1. 16 |
| **Er** | 3. 075 | 3. 75 | 2. 85 | 0. 21 | 2. 3 | 3. 51875 |
| **Tm** | 0. 451 | 0. 63 | 0. 405 | 0. 0324 | 0. 33 | 0. 526667 |
| **Yb** | 3. 012 | 3. 53 | 2. 86 | 0. 209 | 2. 2 | 3. 1546 |
| **Lu** | 0. 4386 | 0. 61 | 0. 43 | 0. 0332 | 0. 32 | 0. 4944 |

The REE values of the samples were normalized to the upper crust (Table 4). Based on this normalization, the samples generally display enrichment in medium rare earth elements (MREEs) (Table 3; Figure 23). When the REE abundances and enrichments relative to the upper crust are evaluated, it is particularly evident that FAR−2, KAZ−7, and BAY−5 show enrichment across all REEs, with FAR−2 exhibiting exceptionally high concentrations (Figure 21 a–d; Figure 24-25).

Table 4. UCC-normalized REE Values.

| Upper crust | La | Ce | Pr | Nd | Sm | Eu | Gd | Tb | Dy | Ho | Er | Tm | Yb | Lu |
|---|---|---|---|---|---|---|---|---|---|---|---|---|---|---|
| **CER2** | 0.062 | 0.162 | 0.068 | 0.050 | 0.089 | 0.188 | 0.153 | 0.088 | 0.089 | 0.072 | 0.071 | 0.034 | 0.071 | 0.084 |
| **CER4** | 0.068 | 0.141 | 0.080 | 0.060 | 0.109 | 0.198 | 0.153 | 0.097 | 0.100 | 0.082 | 0.081 | 0.040 | 0.081 | 0.082 |
| **CER6** | 0.123 | 0.123 | 0.128 | 0.092 | 0.154 | 0.253 | 0.199 | 0.141 | 0.158 | 0.129 | 0.133 | 0.064 | 0.131 | 0.143 |
| **FAR1** | 0.113 | 0.230 | 0.110 | 0.074 | 0.127 | 0.189 | 0.199 | 0.144 | 0.151 | 0.133 | 0.141 | 0.073 | 0.151 | 0.173 |
| **FAR2** | 0.059 | 0.069 | 0.081 | 0.071 | 0.203 | 0.330 | 0.351 | 0.363 | 0.437 | 0.391 | 0.380 | 0.176 | 0.343 | 0.348 |
| **FAR3** | 0.040 | 0.174 | 0.036 | 0.026 | 0.042 | 0.089 | 0.103 | 0.052 | 0.049 | 0.048 | 0.050 | 0.028 | 0.062 | 0.066 |
| **INC1** | 0.032 | 0.029 | 0.037 | 0.028 | 0.050 | 0.099 | 0.078 | 0.051 | 0.056 | 0.042 | 0.042 | 0.021 | 0.038 | 0.042 |
| **INC3** | 0.050 | 0.082 | 0.059 | 0.046 | 0.076 | 0.151 | 0.122 | 0.071 | 0.075 | 0.058 | 0.051 | 0.023 | 0.047 | 0.052 |
| **INC5** | 0.041 | 0.035 | 0.049 | 0.036 | 0.065 | 0.133 | 0.107 | 0.063 | 0.065 | 0.054 | 0.050 | 0.023 | 0.044 | 0.053 |
| **KAZ1** | 0.107 | 0.118 | 0.123 | 0.094 | 0.170 | 0.244 | 0.214 | 0.163 | 0.170 | 0.138 | 0.130 | 0.063 | 0.120 | 0.125 |
| **KAZ4** | 0.056 | 0.065 | 0.063 | 0.048 | 0.085 | 0.137 | 0.123 | 0.094 | 0.096 | 0.085 | 0.083 | 0.040 | 0.080 | 0.085 |
| **KAZ7** | 0.090 | 0.188 | 0.101 | 0.077 | 0.124 | 0.189 | 0.171 | 0.123 | 0.110 | 0.088 | 0.083 | 0.038 | 0.073 | 0.071 |
| **KAZ9** | 0.078 | 0.147 | 0.093 | 0.069 | 0.120 | 0.183 | 0.168 | 0.113 | 0.118 | 0.093 | 0.094 | 0.043 | 0.085 | 0.088 |
| **KAZ10** | 0.056 | 0.081 | 0.063 | 0.049 | 0.085 | 0.149 | 0.133 | 0.082 | 0.086 | 0.075 | 0.071 | 0.032 | 0.067 | 0.068 |
| **AKC1** | 0.036 | 0.082 | 0.035 | 0.024 | 0.038 | 0.130 | 0.117 | 0.037 | 0.033 | 0.030 | 0.029 | 0.015 | 0.030 | 0.029 |
| **AKC4** | 0.100 | 0.229 | 0.103 | 0.074 | 0.126 | 0.229 | 0.233 | 0.124 | 0.122 | 0.104 | 0.102 | 0.050 | 0.102 | 0.106 |
| **AKC7** | 0.079 | 0.198 | 0.083 | 0.058 | 0.099 | 0.212 | 0.202 | 0.093 | 0.086 | 0.071 | 0.067 | 0.033 | 0.067 | 0.070 |
| **BAY1** | 0.035 | 0.042 | 0.036 | 0.027 | 0.047 | 0.104 | 0.091 | 0.051 | 0.049 | 0.041 | 0.038 | 0.019 | 0.035 | 0.038 |
| **BAY2** | 0.025 | 0.026 | 0.025 | 0.019 | 0.030 | 0.068 | 0.063 | 0.032 | 0.034 | 0.029 | 0.025 | 0.013 | 0.025 | 0.029 |
| **BAY5** | 0.113 | 0.197 | 0.115 | 0.084 | 0.139 | 0.212 | 0.200 | 0.134 | 0.122 | 0.097 | 0.090 | 0.043 | 0.081 | 0.082 |

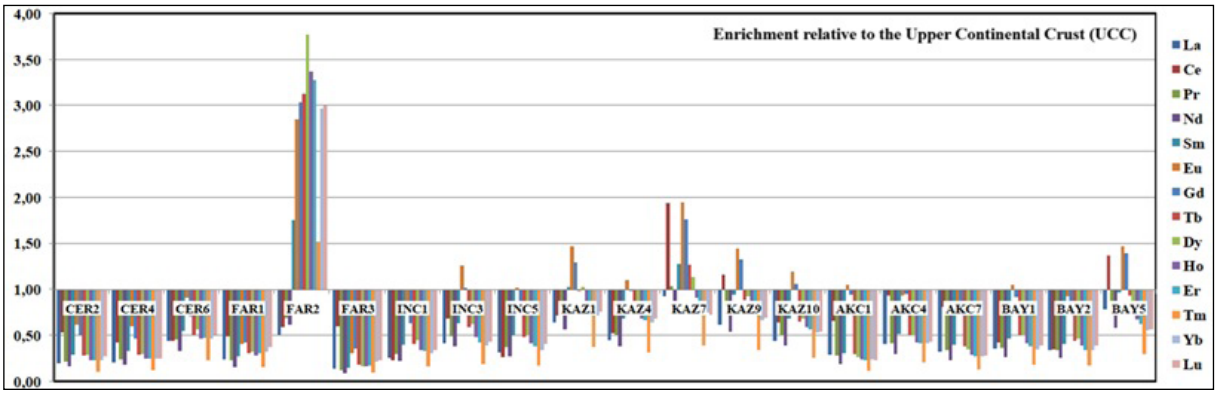


Figure 25- Correlation of REE abundances of all samples normalized to the upper continental crust.

## 5. Conclusions

The mineralogical and geochemical data obtained from the red-colored sedimentary units of the Kazmaca, İncik, and Bayındır formations reveal clear evidence of a multi-phase enrichment process involving both uranium and rare earth elements (REEs), especially the middle REEs (MREEs).

The identification of the secondary uranyl mineral Fourmarierite through XRD and ICP-MS analyses points to post-depositional oxidation processes that played a crucial role in uranium mobilization and subsequent precipitation. This is consistent with the presence of oxidized iron phases ($Fe^{3+}$), which not only impart the red coloration to these formations but also indicate sedimentation under oxygen-rich, low-organic conditions, likely within shallow lacustrine or distal marine environments (Langmuir, 1978; Jahn et al., 1981).

REE distributions normalized to Upper Continental Crust (UCC) values indicate a distinct enrichment of MREEs and heavy REEs (HREEs), especially in samples from the Kazmaca, Bayındır, and Faraşlı areas (e.g., KAZ−7, BAY−5, FAR−2). These enrichments are closely associated with Fe- and Mn-oxyhydroxide phases, which are known to selectively adsorb MREEs under oxidative conditions (Lottermoser, 1990; Sanematsu et al., 2011; 2013). The high Cu/Al ratios and Fe concentrations observed in these samples further support a redox-controlled precipitation model.

Additionally, the clay-rich lithologies, especially fine-grained mudstones and claystones, show geochemical signatures [e.g., elevated Chemical Index of Alteration (CIA), depleted $Na_2O$ and CaO] that are indicative of intense weathering under hot and humid conditions (Bao and Zhao, 2008). Such settings facilitate REE mobilization and their adsorption onto clay surfaces. This process is reminiscent of ion-adsorption-type (IAD) REE enrichment observed in lateritic profiles in South China (Wang et al., 2018; Zeng et al., 2019), suggesting that similar mechanisms may be active in the studied red-bed sequences despite their different depositional context.

The occurrence of microbial activity is also a likely contributing factor to REE mobility, as microorganisms can enhance mineral dissolution and alter redox conditions, thereby indirectly influencing metal enrichment (Banfield and Eggleton, 1989; Taunton et al., 2000). The mineralogical association between clay minerals and secondary uranium phases in Kazmaca and Bayındır suggests that biogeochemical processes may have played a role in the enrichment of REEs.

Collectively, these findings demonstrate that red-bed-type sedimentary systems can host significant REE accumulations driven by a combination of diagenetic redox reactions, weathering, and biogeochemical processes. This study has shown that the red-colored sedimentary formations around Kırıkkale, particularly those in Kazmaca, Bayındır, and Faraşlı, have considerable potential for rare earth element (REE) enrichment in addition to uranium mineralization. The presence of secondary uranium minerals such as Fourmarierite, along with elevated REE concentrations (notably Ce, Nd, Pr, La, Gd, and Dy), underscore the active role of redox conditions in element mobilization and fixation.

Key conclusions include:

• REE enrichment particularly of MREEs and HREEs occurs in association with Fe-oxide and clay-rich lithologies, highlighting the importance of oxidative environments and weathering processes.

• Fourmarierite acts as a mineralogical indicator of uranium mobility under oxidative post-depositional conditions and also reflects favorable conditions for REE adsorption.

• REE concentrations normalized to UCC values in samples such as KAZ−7, BAY−5, and FAR−2 are comparable to those of IAD deposits in South China and lateritic profiles in Japan, suggesting that red-bed units though sedimentary can host REE concentrations of potential economic significance.

• These red-bed units also exhibit elevated Cu/Al ratios, suggesting that base-metal mineralization and REE accumulation may be genetically linked in these settings.

• Given their relatively shallow occurrence and potential for low-cost extraction, these formations should be considered viable targets in Türkiye's strategic mineral-resource exploration.

Overall, red-bed-type sedimentary sequences should be evaluated not only for conventional metals such as copper and uranium but also as strategic REE-bearing systems. Further detailed mineralogical, geochemical, and metallurgical studies are essential to assess their economic feasibility and to guide sustainable, environmentally responsible extraction strategies for Türkiye's future REE supply.

**Acknowledgment**

This study was supported by the Scientific Research Projects Unit of Yozgat Bozok University under the Master's thesis project titled "Rare Earth Element Potential of the Red-Colored Eocene-Aged Kazmaca Formation and Upper Eocene–Lower Miocene-Aged İncik and Bayındır Formations Outcropping Around Kırıkkale" (Project No: FYL-2024-1440).

**Referances**

Alloway, B. J. 2013. Heavymetals in soils: Trace metal sand metalloids in soil sand their bioavailability (Vol. 22). Springer Science and Business Media.

Banfield, J. F., Eggleton, R. A. 1989. Apatite replacement and rare-earth mobilization, fractionation, and fixation during weathering. Claysand Clay Minerals, 37(2), 113–127.

Bao, Z. W., Zhao, Z. H. 2008. Geochemistry of mineralization with exchangeable REY in the weathering crusts of granitic rocks in South China. Ore Geology Reviews, 33(3–4), 519–535.

Birgili, Ş., Yoldaş, R., Ünalan, G. 1975. Çankırı-Çorum havzasının jeolojisi ve petrol olanakları (Report No. 5621). Maden Tetkik ve Arama Genel Müdürlüğü, Ankara (unpublished).

Boynton, W. V. 1984. Geochemistry of Rare Earth Elements: Meteorite Studies. In P. Henderson (Ed.), Rare earth element geochemistry, 63–114. Elsevier.

Brookins, D. G. 1988. Eh-pH diagrams for geochemistry. Springer.

Chakhmouradian, A. R., Wall, F. 2012. Rare earth elements: Minerals, mines, magnets (andmore). Elements, 8(5), 333–340.

Cuney, M., Kyser, K. 2009. Recent and not-so-recent developments in uranium deposit sand implications for exploration. In Mineralogical Association of Canada Short Course, 39, 13–68.

Dahlkamp, F. J. 1993. Uranium ore deposits. Springer.

Dill, H. G. 2010. The geology of aluminum phosphate sand sulphates of the alunite group minerals: A review. Earth-ScienceReviews, 101(1–2), 1–35.

Ding, J. Y. 2012. Historical review of the ionic rare earth mining: In honor of the 60th anniversary of GNMRI. Nonferrous Metals Science and Engineering, 3(4), 14–19. (in Chinese with English abstract).

Finch, R. J., Murakami, T. 1999. Systematic sand paragenesis of uranium minerals. In P. C. Burns and R. Finch (Eds.), Uranium: Mineralogy, geochemistry and the environment, 38, 91–179). Mineralogical Society of America.

Frondel, C. 1958. Systematic mineralogy of uranium and thorium (U.S. Geological Survey Bulletin 1064). U.S. Government Printing Office.

Hakyemez, Y., Barkut, M. Y., Bilginer, E., Pehlivan, Ş., Can, B., Dağer, Z., Sözeri, B. 1986. Yapraklı-Ilgaz Çankırı-Çandır dolayının jeolojisi (Report No. 7966). Maden Tetkik ve Arama Genel Müdürlüğü. [Unpublishedreport, in Turkish].

Henderson, P. 1984. Rare earth element geochemistry. Elsevier.

Jahn, B. M., Glikson, A. Y., Peucat, J. J., Hickman, A. H. 1981. REE geochemistry and isotopic data of Archean silicic volcanic sand granitoids from the Pilbara block, Western Australia—Implications for the early crustal evolution. Geochimica et Cosmochimica Acta, 45 (9), 1633–1652.

Kabata-Pendias, A., Pendias, H. 2011. Trace elements in soil sand plants (4th ed.). CRC Press.

Karadenizli, L.,1999. Çankırı-Çorum Havzasındaki Orta Eosen-Erken Miyosen Tortullarının Sedimantolojisi, Ankara Üniversitesi Fen Bilimleri Enstitüsü Doktora Tezi, 51-195, Ankara.

Karadenizli, L., Saraç, G., Şen, Ş. 2004. Çankırı-Çorum Havzasının Batı ve Güney Kesiminin Memeli Fosillere Dayalı Oligo-Miyosen Biyostratigrafisi ve Dolgulama Evrimi (Rapor No: 10706). Maden Tetkik ve Arama Genel Müdürlüğü (MTA), Ankara (unpublished).

Kynicky, J., Smith, M. P., Xu, C. 2012. Diversity of rare earth deposits: The key example of China. Elements, 8(5), 361–367.

Langmuir, D. 1978. Uranium solution–mineral equilibria at low temperatures with applications to sedimentary ore deposits. Geochimica et CosmochimicaActa, 42(6), 547–569.

Larson, A., Smith, R. D., Johnson, T. E. 2017. Rare earth element fractionation in uranium ore and its U(VI) alteration products. Geochimica et Cosmochimica Acta, 207, 210–223.

Lottermoser, B. G. 1990. Rare-earth element sand ore formation processes. Lithos, 24(2), 151–167.

Lottermoser, B. G. 2010. Mine wastes: Characterization, treatment and environmental impacts (3rd ed.). Springer.

Maden Tetkik ve Arama Genel Müdürlüğü, 2002. 1/500.000 ölçekli Kayseri ve Sinop harita paftası. Ankara.

Morteani, G., Preinfalk, C. 1996. REE distributionand REE carriers in laterites formed on the alkaline complexes of Araxa and Catalo (Brazil). In A. P. Jones, F. Wall, and C. T. Williams (Eds.), Rare earth minerals: Chemistry, origin and ore deposits, 227–252. ChapmanandHall.

Möller, P. 1989. The behavior of rare earth elements in ore formation. In P. Möllerand P. Černý (Eds.), Lanthanides, tantalum and niobium, 121–146. Springer.

Price, R. C., Gray, C. M., Wilson, R. E., Frey, F. A., Taylor, S. R. 1991. The effects of weathering on rare-earth element, Y and Ba abundances in Tertiary basalts from southeastern Australia. Chemical Geology, 93(3–4), 245–265.

Rollinson, H. 1993. Using geochemical data: Evaluation, presentation, interpretation. LongmanScientific and Technical.

Sanematsu, K., Kon, Y., Imai, A., Watanabe, K., Watanabe, Y. 2013. Geochemical and mineralogical characteristics of ion-adsorption type REE mineralization in Phuket, Thailand. Mineralium Deposita, 48(4–5), 437–451.

Sanematsu, K., Moriyama, T., Sotouky, L., Watanabe, Y. 2011. Mobility of rare earth elements in basalt-derived laterite at the Bolaven Plateau, southern Laos. Resource Geology, 61 (2), 140–158.

Taunton, A. E., Welch, S. A., Banfield, J. F. 2000. Microbial controls on phosphate and lanthanide distributions during granite weathering and soil formation. Chemical Geology, 169 (3–4), 371–382.

Wang, D. H., Zhao, Z., Yu, Y., Dai, J. J., Deng, M. C., Zhao, T., Liu, L. J. 2018. Exploration and research progress on ion-adsorption type REE deposit in South China. China Geology, 3(3), 415–424.

Wedepohl, K. H. 1995. The composition of the continental crust. Geochimica et Cosmochimica Acta, 59(7), 1217–1232.

Wronkiewicz, D. J., Buck, E. C. 1996. Uranium mineralogy and geochemistry in the oxidized zone of the Koongarra uranium deposit, Northern Territory, Australia. Applied Geochemistry, 11(5), 571–587.

Xiong, Y., Wang, Z. 2018. Rare earth element partitioning between fluids and uraninite at 50 °C: Implications for secondary REE mineralization. Economic Geology, 113(7), 1345–1358.

Yang, Y. Q., Hu, C. S., Luo, Z. M. 1981. Geological characteristics of mineralization of rare earth deposits of the ion-absorption type and their prospecting direction. Bulletin of the Chinese Academy of Geological Sciences, 2(1), 102–118. (in Chinese with English abstract).

Yavuz Pehlivanlı, B. 2019. The REE characteristics of oil shales in the Lower Eocene Celtek Formation (Yozgat, Türkiye) and their relation to tectonic provenance. Acta Geologica Sinica – English Edition, 93(3), 604–621.

Yavuz Pehlivanlı, B. 2022. Nadir toprak elementlerinin (NTE) maden yataklarında köken belirteci olarak kullanılması. In Anadolu 11th International Conference on Applied Sciences , 1219–1229. Diyarbakır, Türkiye.

Yoldaş, R. 1982. Tosya (Kastamonu) ile Bayat (Çorum) arasındaki bölgenin jeolojisi (Unpublished doctoral dissertation). İstanbul Üniversitesi Fen Fakültesi.

Zeng, K., Li, L. T., Zhu, X. P. 2019. The metallogenic regularity and prospecting potential of rare earth deposits of ion-adsorption type in the Mengwang–Manmai area, Western Yunnan. Geological Exploration, 55(1), 21–31.

Zhu, X., Zhang, B., Ma, G., Pan, Z., Hu, Z., Zhang, B. 2022. Mineralization of ion-adsorption type rare earth deposits in Western Yunnan. Ore Geology Reviews, 148, 104984.